ARTICLE

Research on the Key Technology of High-Performance Nanomaterials for the Enhancement of Mechanical Properties in Modern Industry

Wei Zhang [1,*]

[1] School of Chemistry and Engineering and Technology, Sun Yat-sen University, Guangzhou, 510000

Abstract

Composite of materials is an inevitable law of material development, the so-called composite material is a combination of metal, inorganic non-metal, polymer and other materials into a multi-phase materials, thus giving the composite material lightweight and high strength as well as due to the composite effect of the original components of the superior performance does not have. This paper summarises the role of nanomaterials in strengthening and protection in the field of industrial machinery, lists the reagents and instruments required for the experiments, designs the sealing material culture and prepares the sealing material. The physicochemical characterisation of the composites were extracted and analysed using X-ray powder diffraction and Fourier transform infrared spectroscopy instrumentation respectively. The mechanical properties of the nanocomposites were characterised and analysed from four aspects: tensile properties, impact properties, fracture toughness and dynamic mechanics.The FT-IR characterisation analysis showed that the composite membrane of the nanocomposites showed the collagen C=O stretching vibration peaks at $1658.672 cm^{-1}$ and 1578.669, in which the C=O bond at $1658.672 cm^{-1}$ was a characteristic peak of the secondary structure of the polypeptide. It indicates the presence of protein substances in the hydrolysate of high-performance nanocarbon/epoxy composites. The mechanical properties of the composites were tested, and the flexural strength and flexural modulus of the CNT/epoxy composites increased from 86.24 MPa to 92.484 MPa when the CNT additions were in the range of 5% wt to 15% wt. Therefore, the additions of nanocarbon have an important effect on the flexural strength and flexural modulus of industrial mechanical materials.

*****Corresponding author:**
✉ Wei Zhang
BrainZhang23@gmail.com

[†] These authors contributed equally to this work

1 Introduction

Modern mechanical design and manufacturing process can be divided into two basic aspects of the content, mainly including automation technology for the manufacture of some small and medium-sized machinery and processing machines and the use of special cutting process technology for the processing of mechanical original internal cutting technology [1–3]. Due to the economic development of people's demand for precision performance of industrial machinery products is higher and higher, in the development of industrial machinery manufacturing process people for precision materials and processing technology also further put forward higher requirements and concerns, which is also further realized the healthy and sustainable development of China's machinery manufacturing industry is an important factor and strategy [4–6].

Nanotechnology has been recognized as one of the key technologies of the 21st century. Nanotechnology is the manipulation of matter at the atomic or molecular level, exploring the properties of matter occurring below a certain tiny size in numerous research fields, and is expected to be the basis for the next generation of products [7–9]. The use of special mechanical manufacturing process technology and its corresponding machining process points can realize the precise control and processing of materials and structures, thus improving the performance and function of products [10]. Combining nanotechnology with gas-shielded welding technology can realize highly efficient technical processes such as surface modification, thin-film coating and nanofabrication in order to improve the performance and processing quality of parts [11–14]. Secondly, nanoscale sputter coating technology can form nanometer-thick ceramic, metal, or composite films on the surface of the parts to improve the hardness, wear resistance, and corrosion resistance of the parts, thus increasing the service life and stability of the parts [15–18]. It is foreseeable that advanced materials and nanotechnology will play an increasingly important role in mechanical manufacturing. Future machining processes will further improve the wear resistance, corrosion resistance and surface quality of mechanical equipment to meet the diverse and demanding market needs [19, 20].

In this paper, the physical and chemical properties of nanomaterials are investigated to investigate the strengthening and protection of nanomaterials in the field of industrial machinery. The experimental reagents and experimental apparatus required for the preparation of the materials are listed, the formulation of the sealing materials is designed and the preparation of the sealing materials is carried out sequentially accordingly. The physicochemical properties of the nanocomposites were characterised and analysed using XRD and FT-IR instruments respectively. Meanwhile, the mechanical property characterisation was divided into tensile properties, impact properties, fracture toughness and dynamic mechanics, and the mechanical properties of the composites were characterised and analysed sequentially. Simulation experiments were designed to analyse the microscopic characterization and mechanical properties of high-performance nanocarbon/epoxy composites to summarize the influence of high-performance nanomaterials on industrial mechanical properties.

2 Optimisation of the mechanical properties of modern industry by high-performance materials

2.1 The role of nanomaterials in the optimisation of mechanical properties

Nanomaterials, such as carbon nanotubes and various nanoparticles, are revolutionising the performance of industrial mechanical materials. These materials play a key role in improving the mechanical properties, durability and environmental resilience of industrial materials due to their unique physical and chemical properties [21].

2.1.1 Enhancing mechanical properties: the role of nanomaterial reinforcement

Nanomaterials, have become a key factor in enhancing the mechanical properties of industrial materials. Carbon nanotubes, known for their extraordinary strength and modulus of elasticity, show great potential for reinforcing industrial materials. When these nanoscale tubular structures are embedded in concrete or metallic materials, they can significantly increase the load-bearing capacity of the material. This reinforcing effect stems from the high tensile and compressive properties of carbon nanotubes, which allow composites to withstand greater forces without fracturing. Additionally, due to the lightweight nature of nanomaterials, they can also improve the performance of the material without adding significant weight, which is critical for industrial designs that require a reduction in structural weight without sacrificing strength. Ultimately, the result of the application of this technology is a significant increase in the strength and stability of industrial materials, as well as improved resistance to cracking and vibration.

2.1.2 Enhanced durability: the protective role of nanotechnology

The application of nanotechnology has also greatly improved the durability of industrial materials. In particular, the incorporation of nanoparticles, such as silica nanoparticles, can significantly enhance the compactness and corrosion resistance of concrete. The small size and high activity of silica nanoparticles allow them to be uniformly distributed in the concrete, filling tiny pores and thus reducing the penetration of water and harmful chemicals. This improved concrete is not only stronger, but also more resistant to environmental factors such as water erosion, chemical corrosion and salt damage, significantly extending the service life of industrial properties. In this way, nanotechnology offers the possibility of building more durable and

sustainable industries.

2.2 Preparation of materials

2.2.1 Experimental reagents

Table 1 shows the experimental materials and reagents.

2.2.2 Experimental apparatus

Table 2 shows the experimental apparatus used for the work.

2.3 Experimental methodology

2.3.1 Sealing material formulation design

High-performance nanocarbon/epoxy composites are often used as motive sealing materials in various mechanical equipment, with more excellent airtightness and oil resistance. Therefore, in this experiment, CNT is used as the main rubber material and appropriate amount of reinforcing filler is added to develop a sealing material that can be used in mechanical steel structures [22].

2.3.2 Preparation of sealing materials

1. According to the design of sealing material formula in 2.2.1, weigh the appropriate amount of CNT and other raw materials with an electronic balance.

2. Add the appropriate amount of weighed CNT into the refiner, and carry out the plasticising process for 2min. Then, continue to add an appropriate amount of reinforcing filler, such as nano zinc oxide, etc., into the refiner.

3. Take out the rubber in the refiner and transfer it to the opener. First, set the roller pitch of the opener to 2 mm, and then add an appropriate amount of accelerator for the second mixing process. During the mixing period, cut the rubber every 2 min, and after 20 min of mixing, set the roll spacing of the opener to 1 mm, and carry out the thin pass treatment for 8 times.

4. Set the roll pitch of the opener to 2 mm, take the rubber out of the sheet, and then place the rubber on a clean metal plate and leave it to stand for 16 h in a room temperature environment.

5. Vulcanise the rubber material using a plate vulcanising machine for 15 min at a vulcanising temperature of 165°C. Then take out the vulcanised film, put the material onto a clean metal plate and leave it for 30 min at room temperature to obtain the sealing material.

2.4 Characterisation of physico-chemical properties

2.4.1 X-ray powder diffraction (XRD)

The XRD tests in this paper were realised on a D/Max-2500 X-ray powder diffractometer manufactured by RIKEN, Japan, under the following conditions: the radiation source of the diffractometer was a Cu target line (λ=0.154nm), the scanning speed was 2°/min, and the scanning range was 10~90° [23].

2.4.2 Fourier Transform Infrared Spectroscopy (FT-IR)

In this work, infrared spectroscopy of samples in transmission mode was carried out using a Nicolet iS50 infrared spectrometer from Thermo Fisher Scientific, U.S.A. Specific sizes of the flakes required for the tests were pressed from a small amount of powdered samples mixed homogeneously with potassium bromide (KBr). the resolution of the spectra was $4cm^{-1}$, and the range of scanning wavelengths for the tests was $700 \sim 4000cm^{-1}$ [24].

2.5 Characterisation of mechanical properties of nanocomposites

2.5.1 Tensile properties of nanocomposites

The tensile test of this paper was carried out on the AG-X(10kN) multi-function electronic testing machine of SHIMADZU company in Japan, and the test was conducted according to the national standard GB/T 2567-2008 of the performance test method of the resin casting body, and the test speed was 2 mm/min. The test was carried out using the 1B-type specimen strips, and the test speed was 1 mm/min. The test results were obtained as the tensile strength, the Young's modulus and the elongation at break. The tensile strength, Young's modulus and elongation at break were obtained.

2.5.2 Fracture toughness of composites

In this paper, the test of fracture toughness is carried out in a three-point bending mode with a one-sided notched beam type sample on a multifunctional electronic tester AG-X (10kN) of SHIMADZU, Japan. The dimensions of the specimen are 44 mm × 10 mm × 5 mm, and after casting the specimen of this size, a 5-mm deep notch is cut in the middle of the casting side of the specimen with a super-thin saw blade with a thickness of 0.3 mm. Because the epoxy resin system used in this work is extremely brittle after curing, a lot of attempts to create natural cracks in the notch have failed, so the fracture toughness test work in this paper are carried out in the absence of natural cracks in the specimens. The critical stress field strength factor for type I cracking (i.e., tensile type) was obtained

Material name	Molecular or abbreviation	Purity
Carbon nanotubes	CNT	≥98.0%
nanodiamond	ND	≥99.9%
Graphene oxide	GO	≥99.0%
Activated carbonZX-507	AC	≥99.9%
Epoxy resinzy5401A	$Epoxy$	-
Curing agentzy5401B	-	-
Nitric acid	HNO_3	Primary purity
Hydrogen peroxide solution	H_2O_2/H_2O	30%
Manganese dioxide	MnO_2	≥98.8%
Ammonia water	NH_3H_2O	25~28%
Ferrous nitrite	$Fe(NO_3)_3 \bullet 9H_2O$	≥98.5%
Aluminium ninhydrate	$Al(NO_3)_3 \bullet 9H_2O$	≥99.0%
Ammonium molybdate	$(NH_4)_6Mo_7O_{24} \bullet 4H_2O$	≥99.0%
Orb	$C_6H_8O_7 \bullet H_2O$	≥99.8%
Termethyltrimethyl bromide	$CTAB$	≥99.0%
imidazole	$C_3H_4N_2$	Analytical purity
Anhydrous ethanol	CH_3CH_2OH	≥95.0%
Ammonium polylyate	APP	-
FR CROS 484		
Hydrodiamine phosphate	$(NH_4)_2HPO_4$	≥99.0%
2,2,6,6- tetramemethyl-Nitrogen-Oxides	$TEMPO$	98.6%
Trihydrate copper	$Cu(NO_3)_2 \bullet 3H_2O$	≥98.0%
Potassium carbonate	K_2CO_3	≥99.0%
Hydrogen	H_2	99.99%
Argon gas	Ar	99.99%
10% Ammonia gas	$10\%NH_3/Ar$	Argon gas balance
Deionized water	H_2O	≥18.0$M\Omega cm$

Table 1. Materials and reagents

Device name	Equipment type
Planetary ball mill	QM-3SP2
250ml agate ball mill	-
Household ozone generator	-
Heat type thermostatic heating magnetic stirrer	DF-101S
Four precise electronic balances	CPA224S
Circulating water vacuum pump	SHZ-D
Ultra pure water machine	Master-S
Drying oven	FED 53
The program controls the vacuum drying box	DZF-6020
100mL Hydrothermal reactor	PF2
Electric agitator	JJ-1
Three-roll mill	80E
Stainless steel mould	-
Tube furnace	GSL-1100X-S
Ultrasonic cleaner	SG5200HE
Core funnel	G4
Portable gas tester	8800A

Table 2. Instruments in the research works

at the end of the test (K_{1c}), and the critical strain energy release rate for type I cracking was calculated by combining the Young's modulus with the Poisson's ratio of the epoxy resin (0.34) in accordance with the relationship given in the standard (G_{1c}). Both K_{1c} and G_{1c} reflect the fracture toughness of the material.

2.5.3 Dynamic mechanical analysis of composite materials

The DMA data in this work were obtained on a Dynamic Thermomechanical Analyser Model DMA242E from NETZSCH, Germany, with the following test parameters: single cantilever beam mode, frequency 1 Hz, and ramping rate of 3°C/min from room temperature to 250°C. The glass transition temperature (T_g) was determined by the temperature at which the loss factor ($\tan \delta$) was located on the peak of the temperature profile.In this thesis, G '30 is defined as the energy storage modulus measured at 30°C during the programmed tests.

3 Analysis of mechanical properties of high performance composite nanomaterials

3.1 Microscopic characterisation of nanomaterials

3.1.1 X-ray diffraction analysis

Figure 1 shows the X-ray diffractograms of nano-CNT and high-performance nanocarbon/epoxy composites with different nano-CNT contents in Figure 1(a) and Figure 1(b). For the CG group without nano-CNT addition, diffraction peaks of epoxy resin (PDF#97-002-9151), CoCx (PDF#00-044-0962), $W_{0.12}Co_{0.88}$ (PDF#04-003-2728), and Co_3W_3C (PDF#97-061-7462) can be seen, and the values of the diffraction peaks are 0.621, 0.423, from the left to the right, respectively, 0.185, 0.174, 0.253, and 0.204.

For the high-performance nanocarbon/epoxy composites with the addition of nano-CNT, it can be seen that the diffraction peak of Co_3W_3C (PDF#97-061-7462) in the high-performance nanocarbon/epoxy composites almost disappears starting from CNT 0.3, and the vanishing point is at 38.077°, and the intensity of CNT (PDF#97-015-9879) gradually increases, and then the 2θ is at 46.984° corresponds to the gradual increase of the nano-CNT content. For the epoxy resin without added nano-CNT, there are no other elements solidly dissolved in cobalt that inhibit the diffusion of W and C into Co, and in the carbon-deficient position, W and C diffuse into Co to form the Co_3W_3C-phase. However, when nano-CNT is dissolved in cobalt, the diffusion of W and C into Co is inhibited. As a result, the content of Co_3W_3C in the polycrystalline layer decreases,
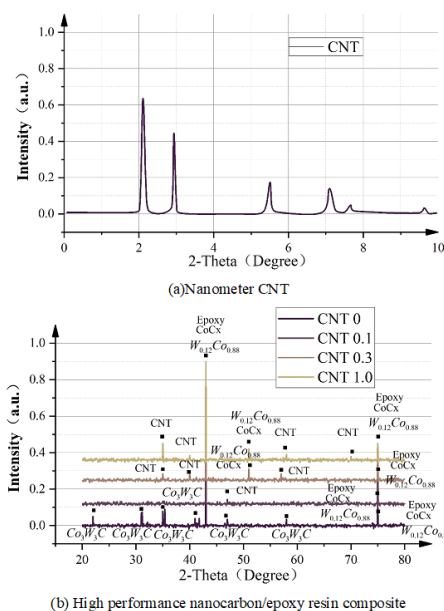

Figure 1. Nano-cnt and high-performance nanocarbon/epoxy resin composites

corresponding to a decrease in the intensity of its diffraction peak. At the same time, the increase in the content of nano-CNT diffused in the cobalt-based binder facilitates the reduction of the contact area between the epoxy resin and the cobalt-based binder.

3.1.2 FT-IR characterisation analysis

In this paper, Fourier transform infrared spectroscopy was used to determine the chemical properties of composite nanofibres and to compare them with PVA nanofibrous membranes. The FT-IR spectra of the two nanofibre membranes are shown in Figure 2. From Figure 2, it can be seen that the characteristic peaks and wave numbers of PVA nanofibre membrane and CNT nanofibre membrane are similar, and at the same time, the characteristic peaks of collagen appeared in the composite membrane, which indicates that the chemical structure of PVA has not been destroyed, and that the chemical structure of collagen has been preserved, suggesting that the PVA and CNT are simple physical Composite. The C=O stretching vibration peaks of collagen appeared in the composite film at 1658.672 and $1578.669 cm^{-1}$, and a weak peak at $3153.568 cm^{-1}$ was caused by the C-H stretching vibration on the unsaturated carbon, which indicated that the CNT contained peptides and proteins, and the C=O bond at $1658.672 cm^{-1}$ was a characteristic peak of the secondary structure of peptides, which further indicated that the high-performance nanocarbon/carbon composite film was a simple physical composite. Peaks, further indicating the presence of protein substances in the
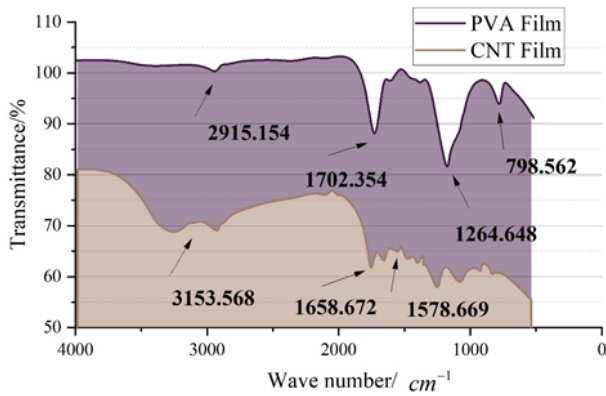
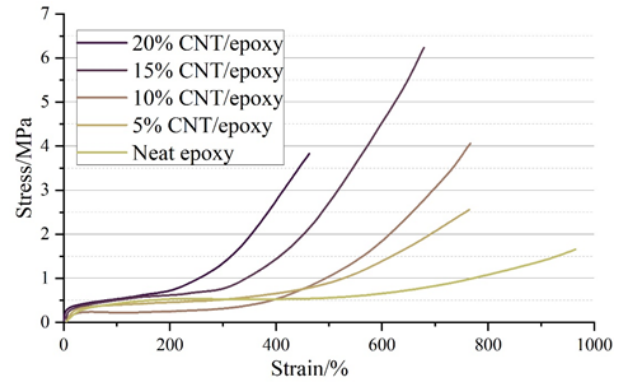**Figure 2.** Two kinds of nano-fiber membrane

Figure 3. Stress-strain curve

hydrolysate of high-performance nanocarbon/epoxy composites.

3.2 Mechanical properties of composite materials

3.2.1 Mechanical Performance Test

1. Stress-strain curve

The stress-strain curves of the high-performance nanocarbon/epoxy composites with different contents are shown in Figure 3, and the corresponding tensile properties are shown in Table 3. The tensile strength of the high-performance nanocarbon/epoxy composites firstly increases and then decreases with the increase of the content of CNT nano-sheets, and the tensile strength of 15% high-performance nanocarbon/epoxy composites is the highest at 6.264MPa, which increases by 280.79% compared with that of pure epoxy at 1.645MPa. The tensile strength of 15% CNT/epoxy composites was the highest, 6.264MPa, which was 280.79% higher than that of pure epoxy, 1.645MPa, and with the increase of CNT nanosheets, the 100% and 300% constant tensile stresses of high-performance nanocarbon/epoxy composites increased, and the 300% constant tensile stress of 20% CNT/epoxy composites was 1.385MPa, which indicated that the compositing of CNT nanosheets with epoxy latex particles achieved a better tensile strength of rubber through physical cross-linking. Physical cross-linking effect achieved the reinforcement of the rubber matrix. However, the addition of rigid lamellar particles CNT nanosheets restricted the movement of rubber macromolecular chains, which led to a decrease in the elongation at break of the composites.

2. Hot air aging performance

Due to the highly saturated nature of the high-performance nanocarbon/epoxy resin itself, both epoxy and CNT/epoxy composites showed excellent hot-air aging resistance. Figure 4 shows the rate of change of mechanical properties of composites after hot air aging. The tensile strength of both epoxy and CNT/epoxy composites decreased to a certain extent after hot air aging at 150°C for 24 h. This is due to the fact that there are still some unreduced C=C double bonds in epoxy, which are prone to be attacked by free radicals and fracture during the hot air aging process, resulting in a decrease of tensile strength. However, the tensile strength of epoxy still maintains the tensile strength respectively. However, the tensile strength still maintains 80% and 85% respectively, which are both at a high level. The CNT/epoxy composites showed better hot air aging resistance due to the good thermal conductivity of CNT, which can transfer the heat generated in the rubber matrix in time. The hot air aging process causes the rubber material to undergo further cross-linking reaction, the cross-linking network of the rubber further increases, the movement of the molecular chain is restricted, and therefore the elongation at break is reduced. However, due to the strong interaction between CNT and epoxy in the CNT/epoxy composite, which already has a high cross-linking density, less cross-linking reactions continue to occur during hot air ageing, and therefore the elongation at break decreases less. Similarly, due to the further cross-linking of the rubber material, the 100% constant elongation stress and 300% constant elongation stress of the epoxy composite are correspondingly increased.

3.2.2 Dynamic thermo-mechanical properties DMA

The energy storage modulus and loss tangent angle of high-performance nanocarbon/epoxy composites with different contents are shown in Figure 5, respectively,

Sample name	Tensile strength/MPa	Elongation of fracture/%	100% definite stress/MPa	300% definite stress/MPa
Epoxy	1.618	987	0.385	0.469
5% CNT/epoxy	2.569	736	0.468	0.458
10% CNT/epoxy	3.766	747	0.439	0.318
15% CNT/epoxy	6.248	699	0.487	0.799
20% CNT/epoxy	3.848	469	0.472	1.385

Table 3. Tensile performance
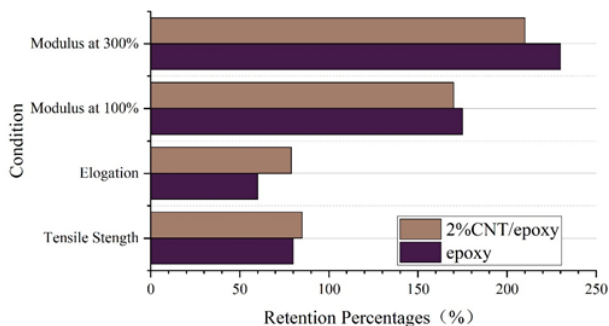
Figure 4. The rate of change of mechanical properties after thermal air aging

Figure 5. High performance nano-carbon/epoxy resin composite materials

Figure 5(a) shows the energy storage modulus, and Figure 5(b) shows the loss tangent angle. From Figure 5, it can be seen that, with the increase of the CNT content, in the high elasticity state of epoxy, the storage modulus of CNT/epoxy composites increases sequentially, and the 15% CNT/epoxy composites have the highest energy storage modulus is the highest, exceeding 1100 MPa, while $\tan\delta$ the peak value decreases sequentially, and the loss factor of 20% CNT/epoxy composites peaks at $1.655\tan\delta$. The glass transition temperature does not change much, i.e., CNT nanosheets grafted on the epoxy molecular chains limit the slip of rubber macromolecules, and the interfacial interactions of the two phases are enhanced, and at the same time, with the assistance of the proteins around the epoxy particles, the An effective transfer of stress from the epoxy molecular chains to the CNT nanosheets was achieved.

3.3 Impact of high-performance nanomaterials on industrial mechanical properties

Figure 6 shows the mechanical property test results of each group of composites, which were subjected to three-point bending test, modified three-point bending test and tensile test for the samples, respectively, Figure 6(a) shows the bending strength, Figure 6(b) shows the bending modulus, Figure 6(c) shows the total work of rupture and Figure 6(d) shows the tensile strength. According to the results of the three-point bending test, as shown in Figure 5(a) and 5(b), it can be seen that when the CNT addition is from 5%wt to 15%wt, the flexural strength and flexural modulus of
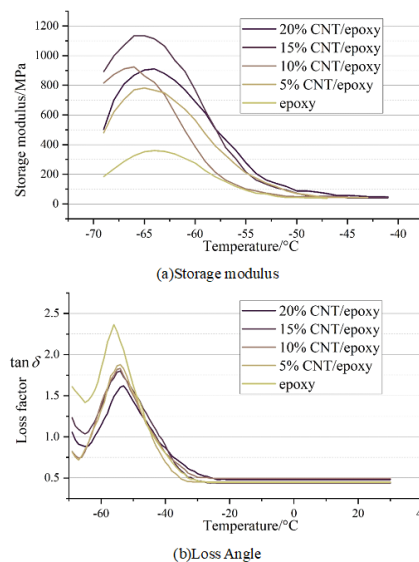
the CNT/epoxy composites are gradually increased from 86.24MPa to 92.484MPa As the CNT content continues to increase, the flexural strength and flexural modulus of the specimens begin to gradually decrease again, where the The flexural strength and flexural modulus of the specimens in the 15%wt group reached the maximum values of 92.484MPa and 2936.654MPa, respectively. Compared with the 15%wt group, the flexural strength and flexural modulus of the 20%wt group decreased significantly. Figure 6(c) shows the results of the modified three-point bending test, and it can be seen that the total work of fracture W_t of the specimens in each group gradually increased when the CNT content was from 0%wt to 10%wt, and the difference was $115.314 J/m^2$ compared with the control group at 0%wt . When CNT increased from 10%W_t to 20%W_t, the W_t of the specimens gradually decreased and reached a maximum value of $615.959 J/m^2$ at 10%W_t group. The statistical results of tensile test of specimens in each group (Figure 6(d)) show that the tensile strength of specimens in the 0%W_t to 15%W_t group shows a gradual increase, and the tensile strength reaches the maximum value of 115.675 MPa in the 15%W_t group, and thereafter, the tensile strength of each test group shows a gradual decrease.
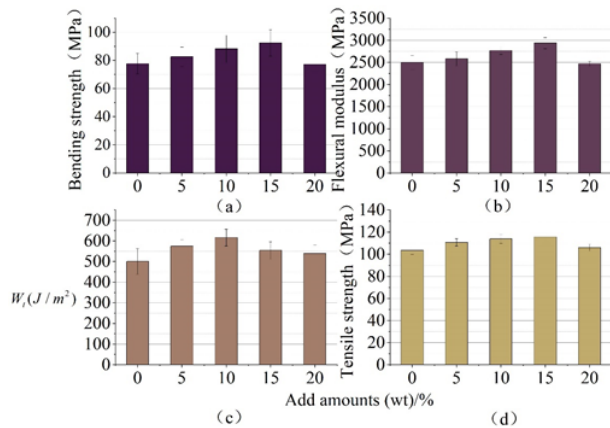
Figure 6. The mechanical ability of each group of composite materials can test the results

4 Conclusion

This paper summarises the role of nanomaterials in the optimisation of mechanical properties, in terms of enhancing mechanical properties and increasing durability respectively. The sealing material formulations were designed and the sealing materials were prepared using experimental reagents and instruments. The prepared composites were analysed for physicochemical property characterisation by X-ray powder diffraction and Fourier transform infrared spectroscopy.

In the X-ray diffraction analysis, the Co_3W_3C diffraction peaks in the high-performance carbon/epoxy nanocomposites almost disappeared starting from CNT 0.3, with the disappearance point at 38.077°, and the intensity of CNT gradually increased, with the growth point at 46.984°. In the FT-IR characterization analysis, comparing the chemical properties of PVA nanofibers and CNT nanofibers, the CNT nanocomposite composite film at 1658.672, 1578.669 appeared the collagen C=O stretching vibration peaks, in which the C=O bond at $1658.672cm^{-1}$ is a characteristic peak of the secondary structure of the peptide, which further indicates that there is a protein substance in the hydrolysate of the high-performance nanocarbon/epoxy composites.

Mechanical analysis of the mechanical properties of the composites showed that the 15% high-performance nanocarbon/epoxy composite had the highest tensile strength of 6.264 MPa, which was enhanced by 280.79% compared to the pure epoxy material, and the 300% constant tensile stress of the 20%-content CNT/epoxy composite reached 1.385 MPa. The CNT nano-sheets and epoxy latex composite achieved the reinforcement of rubber matrix through physical

cross-linking. As the energy storage modulus of CNT/epoxy composites increased sequentially, the 15% CNT/epoxy composites had the highest energy storage modulus of more than 1,100 MPa, but $\tan\delta$ the peak value decreased, and the peak value of loss factor of 20% CNT/epoxy composites was $1.655\tan\delta$.

References

[1] Niu, K. (2024). Research on the Application and Performance of New Materials in Mechanical Manufacturing. *Journal of Engineering Mechanics and Machinery, 9*(1), 121-127.

[2] Morison, E. E. (2016). *Men, Machines, and Modern Times*. MIT press.

[3] Rojek, I., Macko, M., Mikołajewski, D., Sága, M., & Burczyński, T. (2021). Modern methods in the field of machine modelling and simulation as a research and practical issue related to Industry 4.0. Bulletin of the Polish Academy of Sciences. *Technical Sciences, 69*(2), e136717.

[4] Rashid, A. B., Haque, M., Islam, S. M., & Labib, K. R. U. (2024). Nanotechnology-enhanced fiber-reinforced polymer composites: Recent advancements on processing techniques and applications. *Heliyon*, e24692

[5] Zein El-Din, A. M., Youssef Taha, R. M., & Abdel Hamied, R. G. (2021). Nanotechnology sector applications in power and farm machinery: a review. *Journal of the Advances in Agricultural Researches, 26*(2), 38-47.

[6] Talebian, S., Rodrigues, T., Das Neves, J., Sarmento, B., Langer, R., & Conde, J. (2021). Facts and figures on materials science and nanotechnology progress and investment. *ACS nano, 15*(10), 15940-15952.

[7] Malik, S., Muhammad, K., & Waheed, Y. (2023). Nanotechnology: A revolution in modern industry. *Molecules, 28*(2), 661.

[8] Subhan, M. A., Choudhury, K. P., & Neogi, N. (2021). Advances with molecular nanomaterials in industrial manufacturing applications. *Nano Manufacturing, 1*(2), 75-97.

[9] Denisenko, M., Deviatko, O., Kanivets, N., Mushtruk, N., & Tuziuk, M. (2024). Application of Nanomaterials and Nanotechnologies to Increase the Durability of Agricultural Machinery Working Bodies. In *Design, Simulation, Manufacturing: The Innovation Exchange* (pp. 371-381). Cham: Springer Nature Switzerland.

[10] Reverberi, A. P., D'Addona, D. M., Bruzzone, A. A. G., Teti, R., & Fabiano, B. (2019). Nanotechnology in machining processes: recent advances. *Procedia CIRP, 79*, 3-8.

[11] Kuznetsov, M. A., & Zernin, E. A. (2018, August). The current state of application of ultra-and nanostructured powders in technologies in welding technologies. In *Materials Science Forum* (Vol. 927, pp.

20-28). Trans Tech Publications Ltd.

[12] Branagan, D. J., Sergueeva, A. V., Cheng, S., Walleser, J. K., Weznel, T. F., Costa, J. V., ... & Tuffile, C. D. (2013). Strategies for developing bulk materials nanotechnology (BMN) into industrial products. *Materials Science and Technology, 29*(10), 1193-1199.

[13] AlIthari, A. S., Thahab, S. M., & Al-Obbaidi, A. F. (2023). Effect of adding TiO2 nanoparticles on the impact toughness for welding joints of mild steel. *Australian Journal of Mechanical Engineering, 21*(1), 13-26.

[14] Konovalov, S. V., Kormyshev, V. E., Nevskii, S. A., Molotkov, S. G., Ivanov, Y. F., & Gromov, V. E. (2017). Synthesising nanostructural wear-resistant coatings on martensite steel by welding methods. *International Journal of Nanotechnology, 14*(7-8), 627-636.

[15] Mbam, S. O., Nwonu, S. E., Orelaja, O. A., Nwigwe, U. S., & Gou, X. F. (2019). Thin-film coating; historical evolution, conventional deposition technologies, stress-state micro/nano-level measurement/models and prospects projection: A critical review. *Materials Research Express, 6*(12), 122001.

[16] Sáenz-Trevizo, A., & Hodge, A. M. (2020). Nanomaterials by design: a review of nanoscale metallic multilayers. *Nanotechnology, 31*(29), 292002.

[17] Liao, W., Lan, S., Gao, L., Zhang, H., Xu, S., Song, J., ... & Lu, Y. (2017). Nanocrystalline high-entropy alloy (CoCrFeNiAl0. 3) thin-film coating by magnetron sputtering. *Thin Solid Films, 638*, 383-388.

[18] Melnikova, G., Kuznetsova, T., Lapitskaya, V., Petrovskaya, A., Chizhik, S., Zykova, A., ... & Yakovin, S. (2021). Nanomechanical and nanotribological properties of nanostructured coatings of tantalum and its compounds on steel substrates. *Nanomaterials, 11*(9), 2407.

[19] Ramachandran, M., Bhargava, R., & Raichurkar, P. P. (2016). Effect of nanotechnology in enhancing mechanical properties of composite materials. *International Journal on Textile Engineering and Processes, 2*(1), 59-63.

[20] Shalaby, M. N., & Saad, M. M. (2020). Advanced material engineering and nanotechnology for improving sports performance and equipment. *International Journal of Psychosocial Rehabilitation, 24*(10), 2314-2322.

[21] Chandra, P., Rastogi, V., Porwal, M., Saxena, U., Verma, A., Fatma, N., ... & Sachan, N. (2024, October). Utilization of Polymers for the Development of Nanomaterials. In *Macromolecular Symposia* (Vol. 413, No. 5, p. 2400068).

[22] Yazdanparast, R., & Rafiee, R. (2024). A rate-dependent crack bridging model for dynamic fracture of CNT-reinforced polymers. *Engineering Fracture Mechanics*, 110535.

[23] Dong, H., Jacques, S. D. M., Butler, K. T., Gutowski, O., Dippel, A. C., von Zimmerman, M., ... & Vamvakeros, A. (2024). Obtaining parallax-free X-ray powder diffraction computed tomography data with a self-supervised neural network. *npj Computational Materials, 10*(1), 201.

[24] Liu, Y., & Delhom, C. D. (2024). Investigation of Fourier transform infrared spectroscopy potential in cotton fiber micronaire measurement and distribution. *Textile Research Journal*, 00405175241235398.